Arctic Mixed-Phase Cloud Properties Derived from Surface-Based Sensors at SHEBA

MATTHEW D. SHUPE AND SERGEY Y. MATROSOV

Cooperative Institute for Research in Environmental Sciences, University of Colorado, and NOAA/Environmental Technology Laboratory, Boulder, Colorado

TANEIL UTTAL

NOAA/Environmental Technology Laboratory, Boulder, Colorado

(Manuscript received 19 November 2004, in final form 28 July 2005)

ABSTRACT

Arctic mixed-phase cloud macro- and microphysical properties are derived from a year of radar, lidar, microwave radiometer, and radiosonde observations made as part of the Surface Heat Budget of the Arctic Ocean (SHEBA) Program in the Beaufort Sea in 1997–98. Mixed-phase clouds occurred 41% of the time and were most frequent in the spring and fall transition seasons. These clouds often consisted of a shallow, cloud-top liquid layer from which ice particles formed and fell, although deep, multilayered mixed-phase cloud scenes were also observed. On average, individual cloud layers persisted for 12 h, while some mixed-phase cloud systems lasted for many days. Ninety percent of the observed mixed-phase clouds were 0.5–3 km thick, had a cloud base of 0–2 km, and resided at a temperature of −25° to −5°C. Under the assumption that the relatively large ice crystals dominate the radar signal, ice properties were retrieved from these clouds using radar reflectivity measurements. The annual average ice particle mean diameter, ice water content, and ice water path were 93 μm, 0.027 g m^{-3}, and 42 g m^{-2}, respectively. These values are all larger than those found in single-phase ice clouds at SHEBA. Vertically resolved cloud liquid properties were not retrieved; however, the annual average, microwave radiometer–derived liquid water path (LWP) in mixed-phase clouds was 61 g m^{-2}. This value is larger than the average LWP observed in single-phase liquid clouds because the liquid water layers in the mixed-phase clouds tended to be thicker than those in all-liquid clouds. Although mixed-phase clouds were observed down to temperatures of about −40°C, the liquid fraction (ratio of LWP to total condensed water path) increased on average from zero at −24°C to one at −14°C. The observations show a range of ~25°C at any given liquid fraction and a phase transition relationship that may change moderately with season.

1. Introduction

Mixed-phase clouds are an understudied component of global cloudiness and are thus poorly represented in models at all scales (e.g., Sun and Shine 1994; Gregory and Morris 1996; Morrison et al. 2003). Model schemes typically partition cloud phase as a function of temperature; however, the appropriate temperature range over which multiple phases can coexist is in question. A review of model parameterizations shows the lower temperature limit for modeled supercooled liquid to range from −40° (Ose 1993; Del Genio et al. 1996) to −23° (Tiedtke 1993) to −15° (Smith 1990; Boucher et al. 1995) to −9°C (Gregory and Morris 1996), while observations have shown liquid water at temperatures as cold as −30° to −40°C (e.g., Rauber and Grant 1986; Heymsfield et al. 1991; Intrieri et al. 2002; Korolev et al. 2003). The proper partitioning of cloud phase is particularly important considering the unique radiative properties of liquid droplets and ice particles due to differences in refractive indices, sizes, and shapes (Sun and Shine 1994; Gayet et al. 2002). Additionally, the phase composition strongly impacts the cloud precipitation efficiency and lifetime (e.g., Jiang et al. 2000). Mixed-phase parameterization uncertainties have been shown to strongly impact our ability to simulate the present-day climate (Gregory and Morris 1996) and to play a crucial role in climate prediction modeling, such as CO_2-doubling experiments (Sun and Shine 1995). Furthermore, model studies have shown that the im-

Corresponding author address: Matthew Shupe, CIRES/NOAA/ETL, R/ET6, 325 Broadway, Boulder, CO 80305.
E-mail: matthew.shupe@noaa.gov

pacts of different mixed-phase cloud parameterizations on model results are more pronounced at higher latitudes (Sun and Shine 1995).

To further motivate the study of Arctic mixed-phase clouds in particular, these clouds occur frequently and have a strong and important radiative interaction with the ice-covered surface. Aircraft observations in the fall over the western Arctic Basin showed that 90% of the sampled boundary layer clouds were mixed phase (Pinto 1998), while many other in situ aircraft campaigns have noted Arctic mixed-phase clouds (Hobbs and Rangno 1990, 1998; Curry et al. 1997; Gultepe et al. 2000; Pinto et al. 2001; Lawson et al. 2001; Korolev et al. 2003). Intrieri et al. (2002) observed the prevalence of liquid-containing clouds in all seasons and an unexpectedly high fraction of these clouds in the Arctic winter. Even small amounts of liquid water in mixed-phase clouds (i.e., <30 g m^{-2}) can have a dramatic impact on cloud radiative effects (Sun and Shine 1994; Shupe and Intrieri 2004), particularly in the Arctic where clouds participate in the delicate cloud–radiation and sea ice–albedo feedbacks (e.g., Curry et al. 1996). Finally, the thermal effects of clouds are heightened in the Arctic relative to lower latitudes due to a relatively cold and dry atmosphere.

Motivated by the dearth of knowledge on mixed-phase clouds and their particular importance in the Arctic, it is informative to briefly summarize the current understanding of mixed-phase cloud properties and processes. Here, mixed-phase clouds of a stratiform nature are described since these are the most prominent and documented type in the Arctic.

Stratiform mixed-phase clouds are frequently topped by a thin layer of cloud liquid that produces small ice particles that quickly grow and precipitate from the base of the liquid layer (Hobbs and Rangno 1985; Heymsfield et al. 1991; Rauber and Tokay 1991; Pinto 1998; Gayet et al. 2002). The presence of liquid and ice in the same volume is colloidally unstable as the liquid will quickly be taken up by ice (Harrington et al. 1999). Rauber and Tokay (1991) observed that the maintenance of cloud liquid at the top of stratiform mixed-phase clouds requires the cloud condensate supply rate to balance or surpass the mass diffusional growth rate of ice crystals. Through a series of model studies, they provide a set of conditions under which cloud-top liquid can form and persist. Ice crystals must be at a low concentration [i.e., low concentration of ice forming nuclei (IFN)] and small in size, such that they are less efficient at growth through water vapor deposition. Liquid formation is more likely at warmer cloud-top temperatures, but can be present even at low temperatures with a moderate updraft. In general, a sufficient updraft may be developed through cloud-top entrainment of dry air, wind shear, radiative cooling, and/or surface turbulent heat fluxes (Rauber and Tokay 1991; Pinto 1998; Olsson and Harrington 2000). In addition to an updraft, the persistence and stability of cloud-top liquid is supported by the sedimentation or removal of ice crystals (Jiang et al. 2000).

Primary ice particle initiation occurs via contact nucleation of IFN with large supercooled liquid droplets and through condensation–freezing (Hobbs and Rangno 1985; Mossop 1985; Rauber and Tokay 1991). Thus, the rate of initial ice formation is controlled by the shape of the liquid droplet size distribution (DSD), IFN concentrations, the level of supersaturation, and time (e.g., Sun and Shine 1995; Pinto 1998). After ice particles are initiated, they grow at the expense of water droplets due to the preferential deposition of vapor onto ice, which has a lower saturation vapor pressure than liquid water (referred to as the Bergeron–Findeisen mechanism). Aggregation and riming can also play a role in ice particle growth in mixed-phase clouds (Hobbs and Rangno 1985, 1998; Rauber 1987). Although their importance is still unknown, two main mechanisms have been proposed for secondary ice particle production (i.e., multiplication) in some mixed-phase clouds. At temperatures between $-2.5°$ and $-8°$C the Hallett and Mossop (1974) rime-splintering process can occur as ice crystals fracture in response to riming by liquid droplets. At temperatures below about $-10°$C, mechanical fracture due to ice particle collisions can occur (Hobbs and Atkinson 1976; Mossop 1985).

The limited set of observations and studies concerning mixed-phase clouds, particularly in the Arctic, leaves substantial ambiguity in our understanding of these clouds, their properties, and their important mechanisms. Some of these deficiencies may be addressed by examining mixed-phase cloud observations from recent Arctic field programs such as the Surface Heat Budget of the Arctic Ocean (SHEBA) Program (Uttal et al. 2002). The field portion of this project was based on an ice-breaking ship that was frozen into the permanent ice pack of the Beaufort Sea for the full year from October 1997 through October 1998. In cooperation with SHEBA, the First International Satellite Cloud Climatology Program (ISCCP) Regional Experiment-Arctic Clouds Experiment (FIRE-ACE) supported aircraft measurements around the SHEBA research site during the months of April through July 1998 (Curry et al. 2000). Measurements from the SHEBA and FIRE-ACE field campaigns provide a

comprehensive view of Arctic cloudiness in all seasons (Intrieri et al. 2002) and a particularly wealthy set of mixed-phase cloud observations. Shupe et al. (2005) outlined an operational cloud property retrieval suite that combines cloud radar, lidar, dual-channel microwave radiometer, and radiosonde data to classify cloud types and retrieve cloud microphysical properties for the clouds observed at SHEBA. That study specifically focused on single-phase cloud retrievals and provided statistical results on the annual evolution of Arctic single-phase cloud properties. Although methods do not currently exist to operationally retrieve all microphysical properties of mixed-phase clouds, some significant and useful information on these important clouds can be derived from SHEBA measurements, and are the focus of this paper.

2. Identifying and characterizing mixed-phase clouds

a. Instrumentation

Ground-based instruments used in this study are as follows: the millimeter cloud radar (MMCR; Moran et al. 1998), which provided profiles of radar reflectivity, Doppler velocity, and Doppler spectrum width; the microwave radiometer (MWR), which provided estimates of the column integrated liquid water path (LWP) and water vapor amounts; a depolarization lidar, which provided information on cloud phase (Intrieri et al. 2002); and radiosondes, which provided profiles of temperature and humidity. The MWR brightness temperatures at 24 and 31 GHz respond to liquid water only, and the data were reprocessed according to Westwater et al. (2001) to account for improvements in the retrieval of LWP from these brightness temperatures. MWR observations prior to 5 December 1997 suffered from irrecoverable calibration problems and are therefore not used here. All ground-based instruments and their measurements are described in the provided references and summarized in more detail by Shupe et al. (2005).

b. Cloud-type classification using ground-based sensors

Clouds above the SHEBA ice camp were classified as being all ice, all liquid, mixed phase, or precipitating based on the measurements from the above instruments and surface observer logs. An in-depth discussion of the classification method is given in Shupe et al. (2005), while only classification aspects pertinent to mixed-phase clouds are discussed here. Mixed-phase clouds are defined as cloud layers that contain both liquid and ice. Generally, the clouds classified as mixed phase during the SHEBA year were similar to the low-level stratiform clouds described in the introduction. Many mixed-phase clouds also contained embedded regions of liquid (e.g., Hobbs et al. 2001), as identified by the depolarization lidar. The definition used here does not imply that all portions of clouds classified as mixed phase contain both ice and liquid in the same volume.

Although all measurements were subjectively reviewed and combined to determine a cloud classification, the following criteria were typically used to identify mixed-phase clouds: 1) a positive LWP derived from the MWR measurements; 2) cloud temperatures $<0°$C from the radiosonde measurements; 3) radar reflectivity typically >-15 dBZ; and 4) radar Doppler velocity typically >0.5 m s^{-1} at some height in the cloud. In addition, surface-observer logs were used to distinguish periods of snowfall. To a certain degree, cloud structure—for example, the flat-topped, supercooled stratiform cloud layer in Fig. 1—was also helpful for identifying mixed-phase clouds.

Additionally, some unique properties of mixed-phase clouds facilitated their identification. The sphericity of liquid droplets compared to the variety of nonspherical ice particle habits provides a clear distinction between phases by lidar depolarization ratios. Ratios less than 0.11 indicate cloud liquid, while higher ratios indicate ice particles (Sassen 1984; Intrieri et al. 2002). This lidar-based phase-discrimination information also aided in the interpretation of some radar observations of mixed-phase clouds. For example, on 6 May 1998 at SHEBA, lidar depolarization ratios indicated a stratiform liquid cloud layer at about 750 m (all heights are AGL) that precipitated ice crystals (Fig. 1a). In the middle of the day, ice crystals falling from above the boundary layer cloud scavenged the cloud liquid, causing the liquid layer to disappear for about 8 h. The MWR-derived LWP (Fig. 1c), in combination with radiosonde temperature profiles (i.e., Fig. 1d), confirms the presence and absence of supercooled liquid water suggested by the lidar depolarization measurements. Radar Doppler spectrum widths (Fig. 1b), which provide information on the spread of the distribution of particle radial motions with respect to the radar, also show a signature from the liquid at the top of the boundary layer cloud. Wide spectrum widths near cloud top in this case indicate a broadened, and at times bimodal, distribution of Doppler velocities that arises from the presence of both cloud liquid droplets and ice particles in the same volume [see Shupe et al. (2004) for more details on mixed-phase cloud Doppler spectra]. Spectral broadening can also be attributed to turbulence; therefore, the spectral width observations were

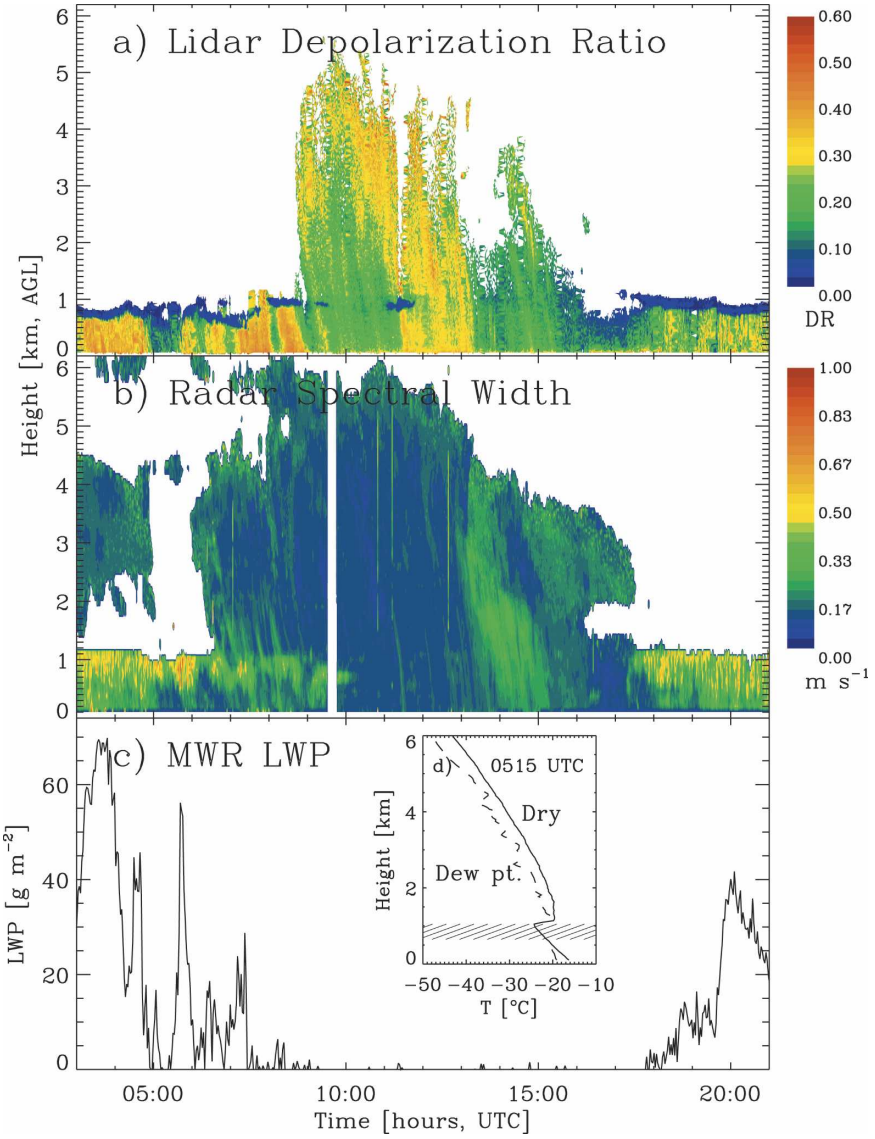

FIG. 1. (a) Lidar depolarization ratio, (b) radar Doppler spectrum width, (c) MWR-derived liquid water path, and (d) dry-bulb and dewpoint temperature soundings at 0515 UTC during a mixed-phase cloud case on 6 May 1998. The heights of the liquid cloud layer at the time of the sounding are indicated in (d).

most often used in conjunction with other supporting information.

c. Cloud property retrievals

Under the assumption of solid particle density, the radar reflectivity, Z_e, is proportional to hydrometeor size to the sixth power. However, for larger ice particles, the effective density is approximately proportional to the reciprocal of size (e.g., Brown and Francis 1995), and hence the radar signal more nearly responds to particle characteristic size to the fourth power (Matrosov et al. 2002). For either case, in most mixed-phase clouds, since ice particles are typically much larger than liquid droplets, the ice component dominates the radar signal (e.g., Gosset and Sauvageot 1992). This assumption has been confirmed by observations of the full radar Doppler spectrum, which showed that even in the presence of substantial liquid water, the ice component of mixed-phase clouds dominates the radar reflectivity (Shupe et al. 2004). In terms of the radar mean Doppler velocity in mixed-phase clouds, Shupe et al. (2004) showed that the ice particles may not dominate the total measured Doppler velocity, which can be biased by the liquid signal and by vertical air motions. The first

bias is substantially reduced under low liquid water conditions, and the second may be reduced by averaging in time. The ice dominance of the radar reflectivity is expected to be particularly true for Arctic mixed-phase clouds since the amount of liquid in Arctic clouds is often small (<100 g m^{-2}; e.g., Lin et al. 2003; Shupe et al. 2005). These small amounts of liquid can emit significant IR radiation however, which inhibits IR radiation-based ice microphysics retrievals (e.g., Matrosov et al. 1992; Mace et al. 1998; Matrosov 1999) from accurately characterizing the ice component of mixed-phase clouds. Similarly, methods that combine lidar and radar observations (Hogan et al. 2003a; Wang et al. 2004) may suffer from lidar attenuation in the liquid portion of mixed-phase clouds (i.e., 0300 to 0900 UTC in Fig. 1). Techniques that are based on radar measurement alone have the potential to yield useful information about the ice component of mixed-phase clouds under most conditions.

Empirical relationships for estimating ice water content (IWC) from Z_e have been explored extensively (Sassen 1987; Liao and Sassen 1994; Atlas et al. 1995; Matrosov 1997), all following the form IWC $= aZ_e^b$, where the coefficients a and b are fixed or fit to the given situation. By assuming a particle density–size relationship (e.g., Brown and Francis 1995), a characteristic ice particle size can then be derived using the same a and b. The retrieved ice particle mean diameter (D_{mean}) reported here is defined as the first moment of the assumed exponential distribution of physical particle sizes, similar to the measurements made by optical in situ probes. Radar-only ice retrievals of this type were applied to all mixed-phase clouds observed at SHEBA using a fixed b coefficient of 0.63 (Matrosov 1999) and an a that varies with season according to statistical results derived from other retrieval methods in single-phase Arctic ice clouds (see Shupe et al. 2005). Thus, the empirical relationships employed here are tuned, in a statistical manner, to the ice particles observed at the SHEBA location. Ice cloud microphysical retrievals have 45-m vertical and 1-min temporal resolution.

Zuidema et al. (2005) provided a detailed description of a mixed-phase cloud from 4 May during SHEBA/FIRE-ACE that included a comparison of aircraft and radar retrievals of cloud properties. Their aircraft data have been used here to expand that comparison to the seasonally varying empirical ice property retrieval [see Zuidema et al. (2005) for more details on the aircraft locations and data processing]. Figure 2 compares aircraft measurements of IWC obtained from multiple horizontal flight legs at different heights over the SHEBA site with radar retrievals for the same times and heights. As in Zuidema et al. (2005), both the mean and standard deviation of retrieval results for the 20-min time period surrounding an aircraft overpass are provided. The comparison demonstrates good agreement, with a relative standard difference (i.e., Matrosov et al. 2002) between the retrieval mean and aircraft data of 51% and a statistical bias of 3%. Comparisons of particle size are not made here due to uncertainties in computing similarly defined sizes. When the same empirical retrieval method was applied to single-phase ice clouds at SHEBA, Shupe et al. (2005) showed uncertainties of as much as 73% for IWC and as much as 40% for D_{mean}. Since the ice component of mixed-phase clouds strongly dominates the radar reflectivity upon which the retrieval is based, the uncertainty in applying this retrieval to mixed-phase clouds is not expected to be drastically different. Additional in situ comparison cases are needed to further characterize the retrieval uncertainties.

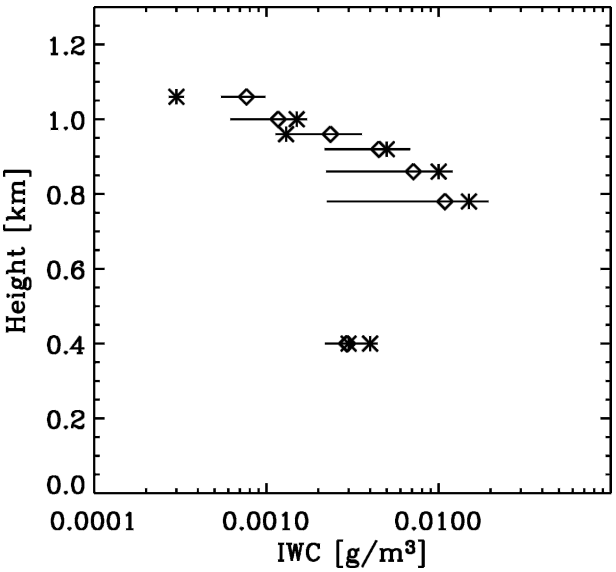

FIG. 2. Comparison of IWC derived from aircraft measurements (asterisks) and radar retrievals (diamonds). Aircraft data are directly from Zuidema et al. (2005). Radar retrievals are given as the mean (diamonds) and standard deviation (horizontal lines) of results for a 20-min time period surrounding the aircraft measurements at a given height.

There were insufficient measurements made by the ground-based sensors at SHEBA to retrieve vertical profiles of the liquid component of all mixed-phase clouds. Various methods for deriving mixed-phase liquid in some clouds have been proposed. One utilizes measurements of the full radar Doppler spectrum (Shupe et al. 2004), which were not regularly recorded at SHEBA. A second method utilizes dual-wavelength radar measurements and differential attenuation (Gos-

set and Sauvageot 1992), although only a single radar was deployed at SHEBA. A third method calculates an adiabatic liquid water profile using the lidar cloud-base measurements and temperature profiles (Zuidema et al. 2005). This retrieval is well suited for single-layer, low-level stratiform mixed-phase clouds, but is difficult to apply to the subset of multilayer mixed-phase clouds observed at SHEBA. Similarly, methods based on IR radiation and/or lidar observations (Turner 2005; Wang et al. 2004) provide useful retrieval information in some cases but may not be applicable to multilayered cloud scenes and may face attenuation effects for optically opaque liquid cloud layers. Thus, since there was no manner to consistently apply any of these methods through the entire SHEBA year, none was used. Instead, the MWR, whose channels at 24 and 31 GHz respond only to liquid water, was used to derive the cloud LWP, which is considered a proxy for the mixed-phase cloud liquid microphysical properties. The uncertainty of LWP retrievals at SHEBA is about 25 g m^{-2} (Westwater et al. 2001).

3. Results

Statistics presented here are for all clouds classified as mixed phase during SHEBA, except where specifically noted. When appropriate, derived mixed-phase cloud properties are compared with similar quantities from the single-phase clouds at SHEBA (presented by Shupe et al. 2005). Retrieved mixed-phase cloud properties are summarized in Table 1. In many figures, box-and-whisker plots are utilized that contain the median (line through the box), 25th and 75th percentiles (edges of box), 5th and 95th percentiles (whiskers), and mean (symbol) of the data.

a. Cloud presence and macrophysical properties

Mixed-phase clouds occurred 41% of the time during the SHEBA annual cycle and 59% of the time that clouds were present. Of the mixed-phase clouds, slightly more than half were the low-level, single-layer, stratiform type described in section 1, while the rest contained multiple layers, were deep, and/or showed evidence of embedded shallow convection. Figure 3a shows the monthly mixed-phase cloud fraction (A_c) over the annual cycle to range from a minimum of ~10% of the time in December to a maximum of 70% in September. There is an indication of more mixed-phase clouds in the spring and fall transition seasons. The transition seasons also exhibit the lowest monthly averaged mixed-phase cloud bases (h_{base} = 0.5 km on average, but more than half of the observed bases were at the lowest radar range gate; Fig. 3b) because in these seasons low-level stratiform mixed-phase clouds with ice crystals extending down to, or near, the surface were the predominant mixed-phase cloud structure. In summer, the average mixed-phase cloud-base height increased to 1–3 km, while in the winter the average base height was about 1 km. Mixed-phase clouds were moderately thinner in May and thicker in midsummer than in other times of the year (Fig. 3c). When considering mixed-phase clouds with temporal breaks in cloudiness of no longer than 1 h, the average persistence of these clouds at SHEBA was greater than 12 h (Fig. 4). The most persistent mixed-phase cloud lasted for 6.4 days; however, one larger-scale mixed-phase cloud system persisted for ~10 days with only moderate (a couple of hours) breaks in the mixed-phase cloudiness.

TABLE 1. Annual mean and range of observations for mixed-phase cloud properties. The range covers the 5th to 95th percentiles of the data for all parameters except A_c, where the range is for monthly averages.

Parameter	Mean	Range
A_c	41%	10%–70%
h_{base}	0.9 km	0–3.5 km
Δh_{cld}	1.9 km	0.4–4.4 km
T_{cld}	−14°C	−27° to −2.3°C
D_{mean}	93 μm	27–200 μm
IWC	0.027 g m^{-3}	10^{-4}–0.11 g m^{-3}
IWP	42 g m^{-2}	0.1–200 g m^{-2}
LWP	61 g m^{-2}	2.2–180 g m^{-2}

The temperature of mixed-phase clouds (T_{cld}, which is derived at each radar range gate, or height level, within the cloud layers; Fig. 3d) varied with season from a monthly average of −25°C in December to a maximum above −10°C in June. The annual and seasonal probability distribution functions (PDF) of mixed-phase cloud temperatures are shown in Fig. 5. For the transition seasons when these clouds occurred most frequently, the majority of cloud temperatures were between −25° and −10°C for spring and −20° and −5°C for fall. The few occurrences of mixed-phase cloud temperatures above 0°C (0.3% of the data) were due to particles falling from mixed-phase layers that encountered warmer temperatures at lower altitudes.

b. Microphysical properties

The characteristic sizes of ice particles in the mixed-phase clouds observed at SHEBA were, on average, smallest in the winter and largest in the summer (Fig. 6a), with an annual average D_{mean} of 93 μm. Retrieved sizes show a gamma-type distribution (Fig. 7a). Low values of mixed-phase IWC and IWP occurred fre-

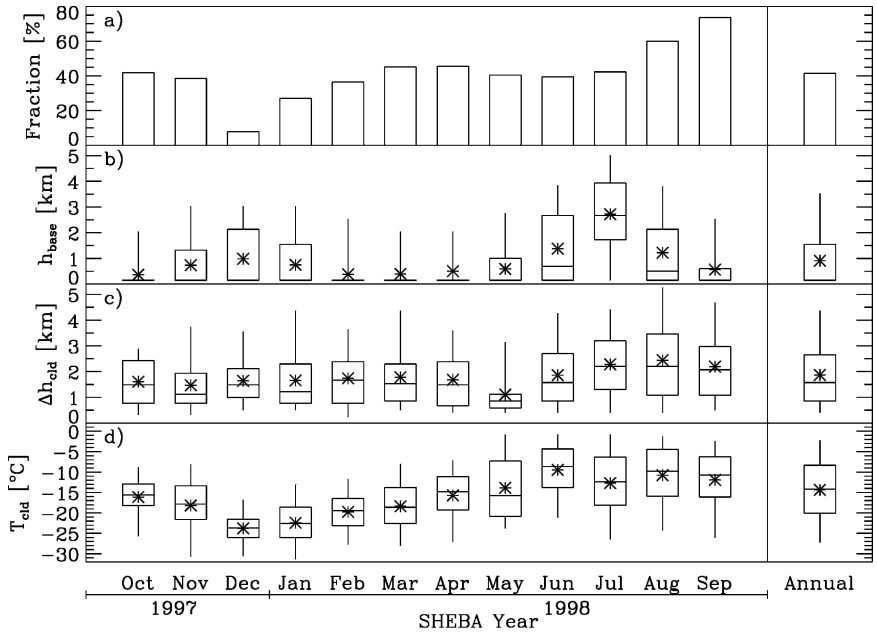

FIG. 3. Monthly and annual mixed-phase cloud statistics of (a) occurrence fraction, (b) cloud-base height, (c) cloud thickness, and (d) cloud temperature. The box-and-whisker plots provide the 5th, 25th, 50th, 75th, and 95th percentiles of the data, and the mean is given as a symbol.

quently in all months (i.e., nearly exponentially distributed; Fig. 7b), and, in general, more large values were observed in the summer and fall (Figs. 6b and 6c). The annual mean IWC and IWP were 0.027 g m^{-3} and 42 g m^{-2}, respectively. Monthly mean mixed-phase cloud LWPs, derived from MWR observations in the subset of single-layer clouds, were at an annual minimum of less than 50 g m^{-2} in winter/spring and a maximum around 100 g m^{-2} in late fall (Fig. 8). The annual mean mixed-phase cloud LWP was 61 g m^{-2}. Since detailed information about the liquid droplet sizes and the vertical distribution of liquid water content were not directly inferred from radar measurements for all mixed-phase clouds, statistics on these quantities are not provided here.

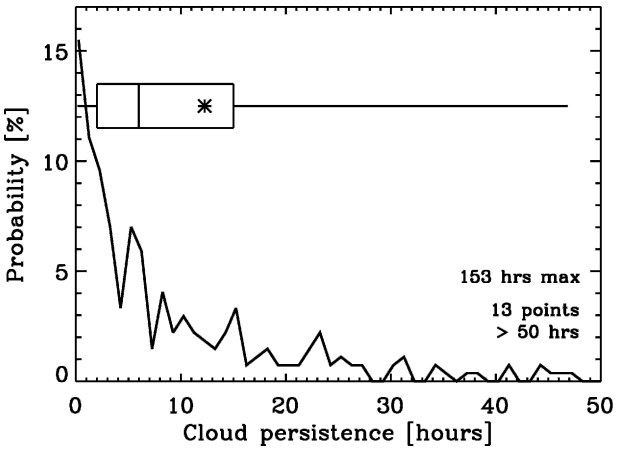

FIG. 4. Probability distribution function of mixed-phase cloud lifetime. Bin sizes are 1 h, and cloud layers with gaps of less than 1 h in duration were considered to be continuous. A total of 284 cloud layers were identified, and the most persistent cloud layer lasted for 153 h or 6.4 days. The box-and-whisker plots provide the 5th, 25th, 50th, 75th, and 95th percentiles of the data, and the mean is given as a symbol.

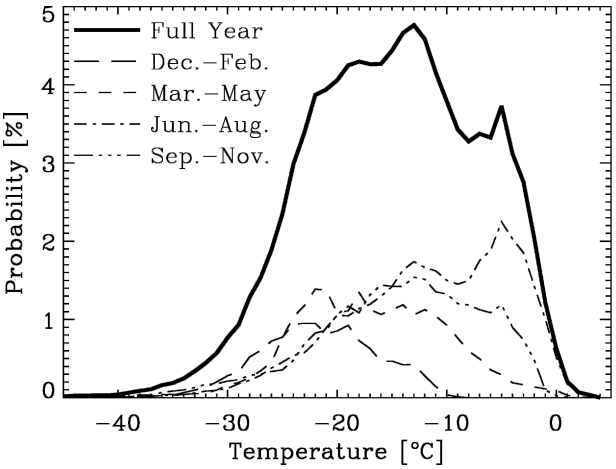

FIG. 5. Probability distribution functions of mixed-phase cloud temperature in 1°C bins.

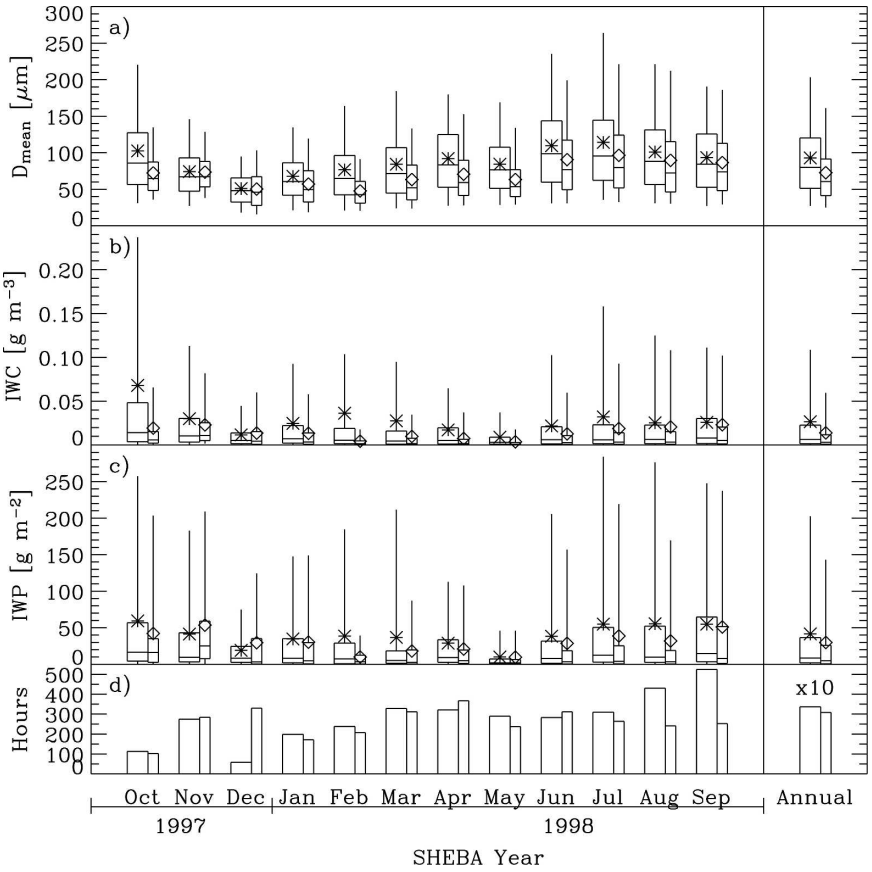

FIG. 6. Monthly and annual statistics of cloud (a) D_{mean}, (b) ice water content, (c) ice water path, and (d) hours of occurrence for mixed-phase (star) and all-ice clouds (diamond). The all-ice cloud results are from Shupe et al. (2005). The box-and-whisker plots provide the 5th, 25th, 50th, 75th, and 95th percentiles of the data, and the mean is given as a symbol.

In general, the mixed-phase clouds observed at SHEBA contained more ice and liquid than single-phase ice or liquid clouds (Figs. 6 and 8; single-phase results are from Shupe et al. 2005). Retrieved mixed-phase ice particle sizes, IWCs, and IWPs are larger than their single-phase counterparts (derived using the same retrieval method) by, on average, 28%, 93%, and 40%, respectively. The relatively small difference in IWP compared to the larger difference in IWC indicates that the mixed-phase clouds were, on average, geometrically thinner than the all-ice clouds. There is a slight suggestion that the differences between mixed-phase and all-ice cloud properties are smallest in the winter when liquid amounts are lowest. Distributions of retrieved properties are similar in shape, but the mixed-phase distributions are weighted more heavily by larger particles and higher IWCs than the single-phase distributions (Fig. 7).

The liquid water paths observed in mixed-phase clouds tended to be slightly larger, in a monthly and annual mean sense, than the LWPs in single-phase clouds (Fig. 8a). The annual mean mixed-phase LWP is 30% larger than the annual mean all-liquid LWP (for the subset of single-layer clouds), with the majority of this difference occurring in the fall and winter months.

Profile statistics were calculated for manually selected cloud layers that were well developed (i.e., not tenuous) and contained only one distinct layer. Thus, multilayered, mixed-phase cloud systems may deviate from the standard profiles discussed here. Cloud profiles were normalized in both cloud depth and parameter value in order to investigate the relative vertical distribution of cloud properties. Statistical analysis was performed on each normalized profile height level. For this reason the monthly and yearly averaged profiles presented here never reach either 0 on the low side or 1 on the high side (which only would be the case if all profiles showed minimum and maximum values at the same normalized height levels).

There are no apparent annual trends in the vertical

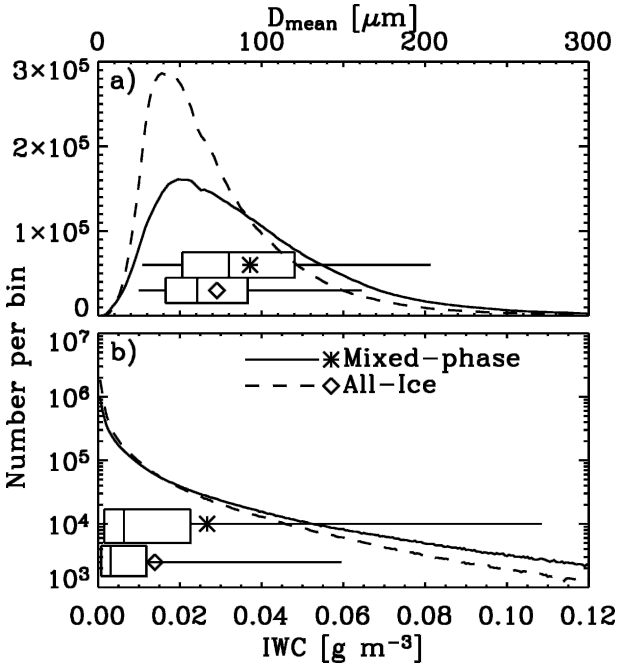

FIG. 7. Annual distributions of retrieved (a) D_{mean} and (b) ice water content for mixed-phase clouds (solid line, star) and all-ice clouds (dashed line, diamond). The all-ice cloud results are from Shupe et al. (2005). The box-and-whisker plots provide the 5th, 25th, 50th, 75th, and 95th percentiles of the data, and the mean is given as a symbol.

distribution of ice within mixed-phase clouds. Figure 9 shows the annual mean normalized profile of mixed-phase cloud IWC, and the profile of the standard deviation. A broad maximum in IWC occurs in the upper-middle portion of the average mixed-phase cloud. Annual averaged profiles of mixed-phase ice D_{mean} are similar to those of IWC. The bulk of the ice mass density was, on average, higher in mixed-phase cloud layers than in all-ice cloud layers (Fig. 9). Furthermore, in mixed-phase clouds, the region of largest ice particle sizes and IWCs was much broader than in all-ice clouds.

c. *Phase partitioning with temperature*

The amount of liquid relative to ice in mixed-phase cloud layers generally increases with cloud-top temperature. Figure 10a shows a scatterplot of cloud-top temperature versus the cloud layer liquid fraction, or the ratio of LWP to total water path (LWP + IWP). All cloud scenes included in Fig. 10 had tops below 5 km and positive values of both LWP and IWP. In general, liquid-dominant mixed-phase clouds at SHEBA had cloud-top temperatures ranging from −25° to 0°C, while ice-dominant clouds had temperatures of −35° to −10°C. At any given liquid fraction, the temperature varied over approximately 20°–25°C. The annual average relationship between the liquid fraction and temperature (Fig. 10) shows a relatively steep decrease in liquid fraction from −14° to −24°C, while there is some indication that the average relationship changed moderately with season. These same data are also visualized in Fig. 11, where the relative probabilities of occurrence for the four quartiles of liquid fraction are given for different cloud-top temperature ranges. At temperatures between −40° and −30°C, 87% of the mixed-phase clouds had liquid fractions of 0 to 0.25, with relatively few occurrences of higher liquid fractions. At suc-

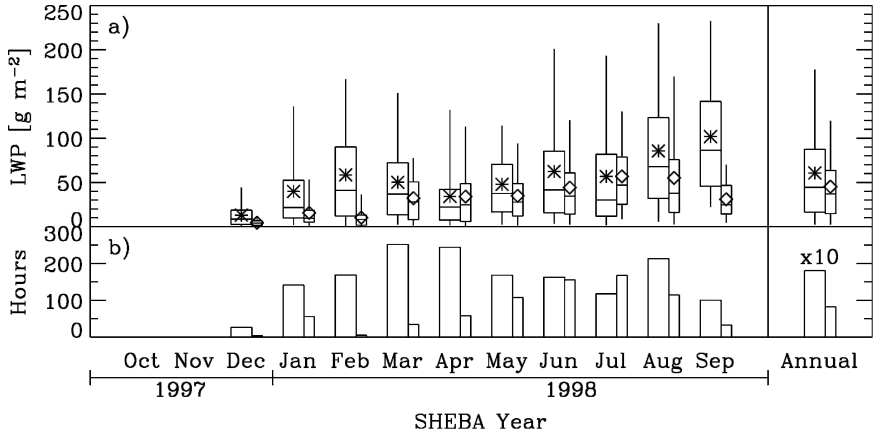

FIG. 8. Monthly and annual statistics of cloud (a) liquid water path and (b) hours of occurrence for single-layer mixed-phase (star) and all-liquid (diamond) clouds. These data are a subset of the full dataset that contained only one liquid-containing cloud type in the vertical column such that the microwave radiometer–derived LWP could be differentiated between mixed-phase and all-liquid clouds. The box-and-whisker plots provide the 5th, 25th, 50th, 75th, and 95th percentiles, and the mean is given as a symbol. MWR data prior to December are not available due to an instrument calibration error.

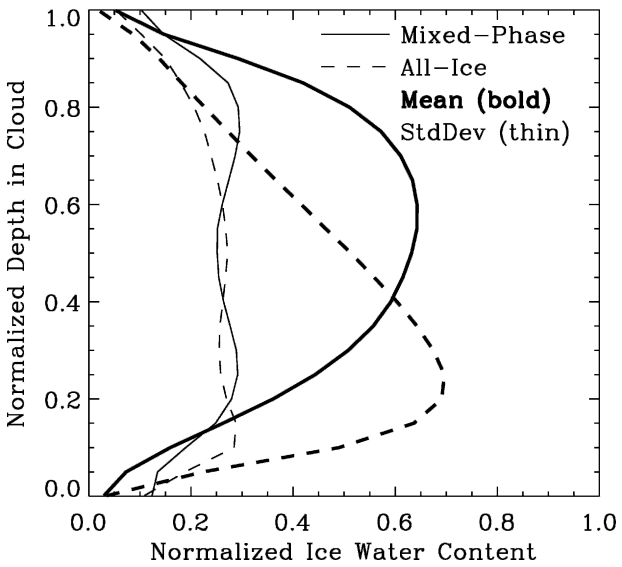

FIG. 9. Annual mean, normalized profiles of retrieved ice water content (bold) and profiles of the standard deviation (thin) for mixed-phase (solid) and all-ice (dashed) clouds. Profiles of particle D_{mean} are similar. The all-ice cloud results are from Shupe et al. (2005).

cessively warmer temperatures, the probabilities of higher liquid fractions increase. Since the cloud top for all clouds discussed in this section was limited to 5 km, the relationships and probabilities presented are most applicable to lower-level mixed-phase clouds that are often of a stratiform nature. Thicker, multilayered mixed-phase clouds may have somewhat different relationships between the liquid fraction and temperature because of the additional impact of ice crystals falling from above liquid cloud layers (i.e., the seeder–feeder mechanism).

4. Discussion

a. Comparison with previous measurements

Arctic mixed-phase clouds have been observed by episodic aircraft missions over the past decade or so; the range of these observations demonstrates the variability of mixed-phase cloud properties. Hobbs and Rangno (1998), Pinto (1998), and Pinto et al. (2001) all observed mixed-phase cloud-base heights and thicknesses to range from a few hundred meters to a few kilometers. Arctic mixed-phase cloud observational datasets have shown temperature ranges of −26° to −6°C (Pinto 1998; Pinto et al. 2001), −21° to −2°C (Hobbs and Rangno 1998), and −40° to 0°C (Korolev et al. 2003). The range of mixed-phase cloud macrophysical properties reported here is consistent with these observations.

In terms of microphysical properties, the variations among observations can be large. Hobbs and Rangno (1998) summarize measurements made over the Beaufort Sea in April 1992 and June 1995 with mixed-phase cloud LWPs as much as ~130 g m^{-2} and most observations less than 60 g m^{-2}. Their IWP values were no more than ~10 g m^{-2}. During the Beaufort and Arctic Storms Experiment (BASE) in the fall of 1994, Pinto (1998) and Pinto et al. (2001) measured boundary layer mixed-phase cloud LWPs of 16–70 g m^{-2} and midlevel LWPs of ~11 g m^{-2}. For ice properties, IWCs of as

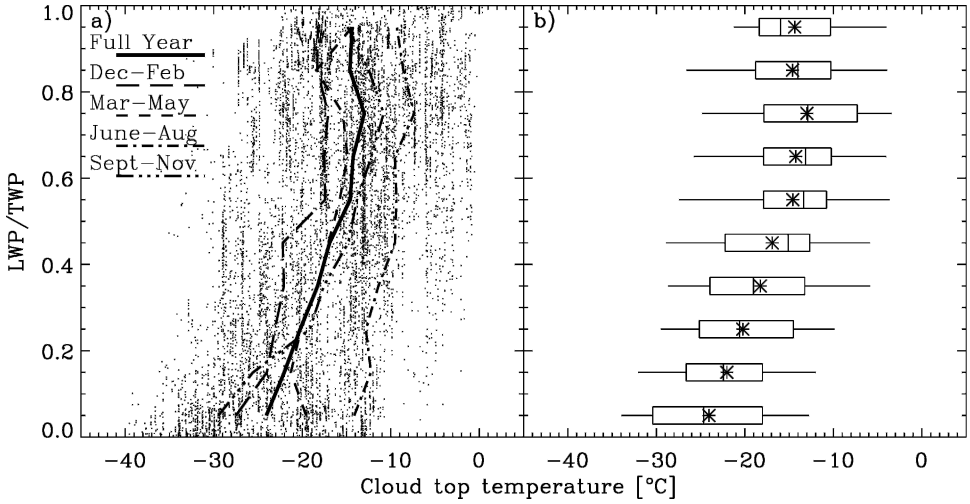

FIG. 10. (a) Scatterplot of the liquid fraction [LWP/(LWP + IWP)] vs cloud-top temperature for mixed-phase clouds. Also plotted are the annual and seasonal average relationships. (b) Box-and-whisker plots summarizing the same data used in (a). The 5th, 25th, 50th, 75th, and 95th percentiles and mean value are provided.

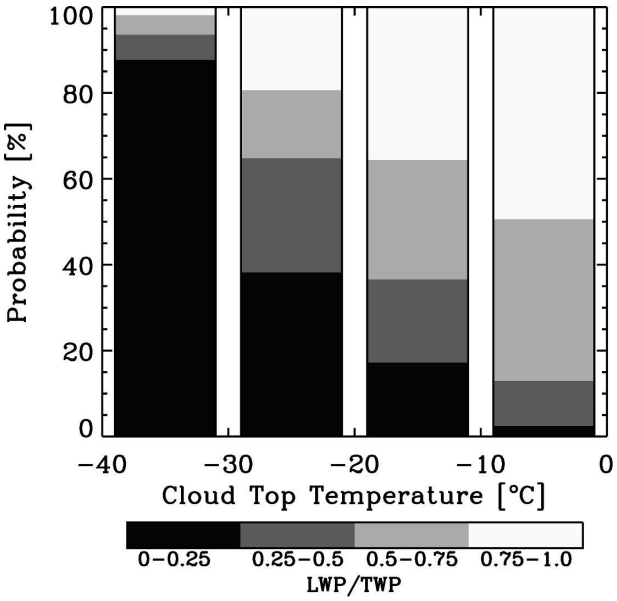

FIG. 11. The relative probabilities of four distinct ranges of the liquid fraction [LWP/(LWP + IWP)] given a cloud-top temperature. For each column, the sum of probabilities for the four possible categories equals 100%.

much as 0.09 g m^{-3} but typically less than 0.01 g m^{-3} were observed, as well as ice particle effective radii of 100–220 μm (D_{mean} of 66–145 μm). Also at BASE, but from a different aircraft, Gultepe et al. (2000) reported average mixed-phase IWCs of 0.02–0.09 g m^{-3} and particle effective radii of 44–54 μm (D_{mean} of 29–36 μm). During May and June at FIRE-ACE, Hobbs et al. (2001) reported mixed-phase cloud LWPs of up to 31 and 68 g m^{-2} for two different case studies and show IWCs typically $<$0.04 g m^{-3} with spikes of as much as 0.06 g m^{-3}. In general, these in situ observations tend to support the range of retrieved microphysical properties, with a few exceptions. The retrievals of IWP reported here are, on average, larger than those reported by Hobbs and Rangno (1998). Also, the BASE in situ observations reported by two different groups show some discrepancies among themselves: the retrievals presented here agree quite well with observations made by Pinto and colleagues, but show some differences from the Gultepe et al. (2000) observations in winter storms. Nonetheless, these in situ observations suggest that the average mixed-phase microphysical properties reported here are within a reasonable range of past in situ observations.

b. *Differences between mixed- and single-phase clouds*

The fact that both the magnitude of ice microphysical properties and their vertical distribution differ between mixed-phase and all-ice clouds indicates that there are marked differences in the particle formation and growth mechanisms, and the total moisture available for particle growth, between these two cloud types. Cirrus clouds (ice only), to a large extent, grow by diffusional growth from water vapor and the growth rates are dependent upon the supply of vapor and the temperature (Pruppacher and Klett 1980), among other properties, which are both relatively low at the higher altitudes where these clouds are found. All of the microphysical mechanisms that are active in cirrus clouds can also play a role in mixed-phase clouds; however, there are additional conditions and mechanisms that promote more rapid ice growth in mixed-phase clouds. Ice particles can grow relatively faster due to the additional moisture at lower and warmer altitudes: Compared to the mixed-phase cloud temperatures shown in Fig. 3d, the all-ice clouds observed at SHEBA were, on average, much colder, with a mean temperature of −31°C and a temperature range (5th to 95th percentiles) of −49° to −14°C. In addition, the Bergeron–Findeisen mechanism, under which ice particles grow at the expense of liquid droplets, plays a major role in mixed-phase clouds. The presence of liquid water drops in these clouds can also invoke the ice initiation and growth mechanisms of contact freezing, condensation freezing, immersion freezing, and riming of ice and snow (e.g., Cooper and Vali 1981; Hobbs and Rangno 1985; Rauber and Tokay 1991; Pinto 1998) that can cause ice particles to grow more rapidly than through vapor deposition alone. Various studies (Harrington et al. 1999; Korolev and Isaac 2003; Khvorostyanov et al. 2003) have suggested that the Bergeron–Findeisen mechanism is the dominant pathway for glaciation in mixed-phase clouds.

The vertical profiles of ice microphysical properties (Fig. 9) also suggest that the growth of ice in mixed-phase clouds is largely tied to the presence of liquid water. For all-ice clouds, the ice particles and IWC grow throughout the top 75% of the cloud layer, while sublimation occurs only in a thin layer near the cloud base. In contrast, mixed-phase cloud ice growth occurs in the top 1/3 of the average cloud layer with a broad maximum in the upper-middle portion of the cloud layer. This profile shape is consistent with in situ observations made by Hobbs and Rangno (1985) and can be attributed to the presence of liquid water near the tops of these clouds.

In spite of these process considerations, these data reveal no significant direct correlation between the total ice and liquid water paths in the mixed-phase clouds observed at SHEBA. Korolev et al. (2003), who also observed no correlation between these parameters,

suggested that since these clouds are typically supersaturated with respect to ice but not necessarily with respect to liquid, the ice particles grow whether or not the liquid droplets also grow.

These data reveal that the average LWP of mixed-phase clouds observed at SHEBA was larger than the average LWP observed in all-liquid clouds. However, the data also indicate that this disparity may be due to differences in liquid cloud layer thickness (and thus vertical motion) instead of differing droplet formation/growth mechanisms. For the subsets of mixed-phase and all-liquid clouds that were single layer and below 5 km, the annual mean LWPs were 43 and 23 g m^{-2}, respectively. Using lidar measurements to derive the base of the liquid layers in these clouds (which are typically somewhat above the base of the cloud ice) and the radar to derive cloud-top heights (e.g., Intrieri et al. 2002), the mean liquid cloud layer thicknesses for stratiform mixed-phase and all-liquid clouds were 620 and 350 m, respectively. Although the liquid water content was not directly retrieved from these clouds, these statistics together suggest that the mean liquid water contents for this subset of mixed-phase and all-liquid clouds were approximately the same: 0.069 and 0.066 g m^{-3}, respectively. Therefore, although the mixed-phase clouds contained, on average, more liquid water than the all-liquid clouds, both of these cloud types contained approximately the same amount of liquid water per vertical extent. Lin et al. (2003) suggest, based on spring and summer observations at SHEBA, that the apparent observed increase of cloud LWP with temperature was actually due to increases in cloud thickness. Their analysis, however, was primarily focused on all-liquid clouds (this dataset confirms their findings of an increased cloud thickness, and thus LWP, with increasing temperature for all-liquid clouds). However, although the data presented here show the same relationship between LWP and cloud thickness in mixed-phase clouds, the temperature trends do not agree with those suggested by Lin et al. (2003) for all-liquid clouds. For the single-layer cloud comparison dataset, the average cloud temperatures were about −17.5° and −11.5°C for mixed-phase and all-liquid clouds, respectively. Thus, the thicker layers of cloud liquid (with higher LWPs) in mixed-phase clouds, compared to all-liquid clouds, were not due to warmer temperatures. Although the mechanism for these differences is currently unknown and will require further investigation, Hobbs and Rangno (1985) made a similar observation that ice-producing altocumulus clouds were often thicker and longer-lived than non-ice-producing altocumulus.

c. Temperature and radiation considerations

Temperature plays a key role in determining mixed-phase cloud occurrence and composition. The fact that mixed-phase clouds tend to occur more frequently in the spring and fall transition seasons (Fig. 3a) suggests that the temperature range during these seasons is most conducive to the coexistence of multiple cloud phases. Radiation may also play a role, since the shortwave (SW) radiative warming of the cloud top decreases at low sun angles, allowing for a relatively larger longwave (LW) radiative cooling to drive the updrafts that are necessary to form and sustain the liquid water in these clouds (i.e., Rauber and Tokay 1991; Pinto 1998; Harrington et al. 1999).

The relationship between temperature and liquid fraction in mixed-phase clouds is particularly important for climate models. The data presented in Figs. 10 and 11 suggest a general trend toward higher liquid fractions at warmer temperatures with a substantial amount of variation in temperature at any given liquid fraction. The increase of the liquid fraction with temperature is predominantly due to increases in LWP with temperature (i.e., Clausius–Clapeyron) and less due to decreases in IWP with temperature. On average, the retrieved mixed-phase cloud ice properties changed very little with cloud temperature over the range of −40° to −10°C (not shown). In support of these findings, other studies have documented the increase in LWP with temperature in the Arctic (e.g., Gultepe and Isaac 1997; Lin et al. 2003). Additionally, Korolev et al. (2003) also observed that mixed-phase cloud IWC did not significantly vary with temperature.

The data in Figs. 10 and 11 are supported by previous observations of phase partitioning with temperature, yet the spread of available observations is large. Differences in the temperature–phase relationship may be expected as the conditions that impact this relationship differ regionally, and likely seasonally, based on sources of moisture, ice-forming nucleus type and concentration, vertical motion, and the net cooling rate (e.g., Pinto 1998). These data, in agreement with other observations (e.g., Heymsfield et al. 1991; Gultepe and Isaac 1997; Hogan et al. 2003b; Korolev et al. 2003), indicate that liquid water occurs at temperatures much colder than some model parameterizations allow (i.e., Moss and Johnson 1994; Smith 1990), and support parameterizations that are able to form cloud liquid at temperatures as low as −40°C. Finally, these observations show a range of about 25°C at any given liquid fraction and a phase transition relationship that may change with season, both of which complicate the ability to accurately parameterize the partitioning of cloud

phases based on temperature alone. None of the parameters presented here (cloud height and thickness, total LWP or IWP) could explain the observed spread in this relationship. Thus, cloud phase parameterizations based on additional parameters (e.g., Tremblay et al. 1996), such as IFN concentrations or vertical motions, will likely be necessary to capture the natural variability of Arctic cloud phase distributions.

5. Conclusions

Mixed-phase clouds occur with relatively high frequency in all seasons in the Arctic, and the partitioning of phases in these clouds has a significant influence on the surface radiation balance. These clouds are poorly modeled due to insufficient knowledge about their structure and formation and persistence mechanisms. Here, an annual cycle of measurements from radar, lidar, microwave radiometer, and radiosondes is utilized to both identify Arctic mixed-phase clouds and to estimate many of their macro- and microphysical properties. All measurements were made as part of the Surface Heat Budget of the Arctic Ocean Program in 1997–98, which provided a particularly useful platform for monitoring mixed-phase cloudiness. The retrieval framework from which these cloud properties were derived, including a detailed assessment of single-phase cloud retrievals and results from SHEBA, is presented in Shupe et al. (2005).

Although a full characterization of Arctic mixed-phase clouds is not possible using the measurements made at SHEBA, there is substantial information on many mixed-phase cloud macro- and microphysical properties. Cloud height, thickness, persistence, and temperature are derived directly from radar measurements and interpolated temperature soundings. Ice microphysical properties are derived from radar reflectivity measurements under the assumption that the large ice crystals dominate the radar signal from these clouds. The coefficients for these ice property retrievals are derived from SHEBA observations and vary by month. There were insufficient measurements to derive vertically resolved cloud liquid properties; however, microwave radiometer retrievals of LWP were useful for characterizing the total liquid water present in mixed-phase clouds.

Major conclusions concerning the macro- and microphysical properties of Arctic mixed-phase clouds include the following:

- Mixed-phase clouds occurred 41% of the time during the SHEBA annual cycle, and 59% of the time that clouds were observed. The annual minimum monthly fraction was 10% in December and the maximum was 70% in September. The majority of mixed-phase clouds occurred in the spring and fall transition seasons. About half of the mixed-phase clouds observed at SHEBA consisted of a single shallow, cloud-top liquid layer from which ice particles formed and fell.
- On average, mixed-phase cloud layers persisted for 12 h. However, many mixed-phase cloud systems persisted for multiple days with only minor intermediate breaks in mixed-phase cloudiness.
- Mixed-phase clouds occurred at temperatures ranging from −40° to 0°C, with most observations from −25° to −5°C. These clouds were typically ~1–3 km thick with a cloud base near the surface.
- Annual mean mixed-phase microphysical properties are $D_{\text{mean}} = 93\ \mu\text{m}$, IWC = 0.027 g m^{-3}, IWP = 42 g m^{-2}, and LWP = 61 g m^{-2}. These are all larger than the equivalent single-phase cloud properties from SHEBA presented by Shupe et al. (2005).
- Ice particle sizes and IWC reach a broad maximum in the upper-middle portion of the average single-layer mixed-phase cloud, somewhat higher within the cloud than for single-phase ice clouds. This profile shape, and its difference from single-phase ice clouds, is likely associated with the liquid water source near the cloud top.
- The liquid fraction, or the ratio of liquid water to total condensed water, generally increases with temperature. The annual average relationship transitions from full glaciation at −24°C to complete liquid water at −14°C, although at any given liquid fraction there is a 25°C range of observed temperatures. The temperature range over which this phase transition occurs may change moderately with season.

The results presented here are useful in that they provide information on the relative trends and magnitudes of mixed-phase cloud properties over a full year in the Arctic. They also reveal how hydrometeor properties are impacted by the presence of two phases as opposed to one, suggesting the important role that additional particle growth mechanisms based on the presence of liquid water can play in shaping the cloud microphysical properties.

Considerable work and new measurements are needed to produce a more complete characterization of Arctic mixed-phase cloud properties. Retrieval methods can be developed, improved, and better validated. For example, radar reflectivity–Doppler velocity methods (Matrosov et al. 2002; Mace et al. 2002) may prove to be more accurate for retrieving mixed-phase ice properties since they are constrained by more measurements; however, these methods must be implemented

with various corrections that may require full radar Doppler spectra. Furthermore, a vertically resolved characterization of the liquid component of these clouds may also require Doppler spectra measurements (Shupe et al. 2004), a profiling multichannel microwave radiometer, or a combination of different retrieval methods based on multiple measurements (i.e., Turner 2005; Wang et al. 2004). Additional study is also necessary to determine how representative the SHEBA annual cycle is of Arctic mixed-phase cloudiness in general, and to specifically investigate why more cloud ice and liquid occur in mixed-phase clouds than in single-phase clouds. Finally, a broader analysis involving more parameters will be necessary to further constrain the cloud phase–temperature relationship in order to improve model phase partitioning parameterizations. These issues may be addressed by new measurements at the Atmospheric Radiation Measurement Program's North Slope of Alaska site, and specifically with data from the Mixed-Phase Arctic Clouds Experiment (fall 2004). Focused in situ aircraft and ground-based remote sensor studies of this nature are needed to further characterize mixed-phase cloud properties and to clarify the mechanisms for mixed-phase cloud formation and persistence.

Acknowledgments. This work was supported by the NSF SHEBA (OPP-9701730), the NASA FIRE-ACE (L64205D), the NASA EOS Validation (S-97895-F), the Department of Energy Office of Science (DE-FG02-05ER63965), and NOAA SEARCH programs. Microwave radiometer data were obtained from the Atmospheric Radiation Measurement Program sponsored by the U.S. Department of Energy. Radiosonde data were obtained from the SHEBA Project Office at the University of Washington Applied Physics Laboratory (UW/APL). The SHEBA project was greatly aided by the logistics team from the UW/APL and the crew of the Canadian Coast Guard Ship *Des Grosseilliers*. We acknowledge the comments of a reviewer whose suggestions strengthened the manuscript.

REFERENCES

Atlas, E., S. Y. Matrosov, A. J. Heymsfield, M.-D. Chou, and D. B. Wolff, 1995: Radar and radiation properties of ice clouds. *J. Appl. Meteor.,* **34,** 2329–2345.

Boucher, O., H. Le Treut, and M. B. Baker, 1995: Precipitation and radiation modeling in a GCM: Introduction of cloud microphysical processes. *J. Geophys. Res.,* **100,** 16 395–16 414.

Brown, P. R. A., and P. N. Francis, 1995: Improved measurements of the ice water content in cirrus using a total-water probe. *J. Atmos. Oceanic Technol.,* **12,** 410–414.

Cooper, W. A., and G. Vali, 1981: The origin of ice in mountain cap clouds. *J. Atmos. Sci.,* **38,** 1244–1259.

Curry, J. A., W. B. Rossow, D. Randall, and J. L. Schramm, 1996: Overview of Arctic cloud and radiation characteristics. *J. Climate,* **9,** 1731–1764.

——, J. O. Pinto, T. Benner, and M. Tschudi, 1997: Evolution of the cloudy boundary layer during the autumnal freezing of the Beaufort Sea. *J. Geophys. Res.,* **102,** 13 851–13 860.

——, and Coauthors, 2000: FIRE Arctic Clouds Experiment. *Bull. Amer. Meteor. Soc.,* **81,** 5–30.

Del Genio, A. D., M.-S. Yao, W. Kovari, and K. K.-W. Lo, 1996: A prognostic cloud water parameterization for global climate models. *J. Climate,* **9,** 270–304.

Gayet, J.-F., S. Asano, A. Yamazaki, A. Uchiyama, A. Sinyuk, O. Jourdan, and F. Auriol, 2002: Two case studies of winter continental-type water and mixed-phase stratocumuli over the sea. 1. Microphysical and optical properties. *J. Geophys. Res.,* **107,** 4569, doi:10.1029/2001JD001106.

Gosset, M., and H. Sauvageot, 1992: A dual-wavelength radar method for ice-water characterization in mixed-phase clouds. *J. Atmos. Oceanic Technol.,* **9,** 538–547.

Gregory, D., and D. Morris, 1996: The sensitivity of climate simulations to the specification of mixed phase clouds. *Climate Dyn.,* **12,** 641–651.

Gultepe, I., and G. Isaac, 1997: Liquid water content and temperature relationship from aircraft observations and its applicability to GCMs. *J. Climate,* **10,** 446–452.

——, ——, D. Judak, R. Nissen, and J. W. Strapp, 2000: Dynamical and microphysical characteristics of Arctic clouds during BASE. *J. Climate,* **13,** 1225–1254.

Hallett, J., and S. C. Mossop, 1974: Production of secondary particles during the riming process. *Nature,* **249,** 26–28.

Harrington, J. Y., T. Reisen, W. R. Cotton, and S. M. Kreidenweis, 1999: Cloud resolving simulations of Arctic stratus. Part II: Transition-season clouds. *Atmos. Res.,* **51,** 45–75.

Heymsfield, A. J., L. M. Miloshevich, A. Slingo, K. Sassen, and D. O'C. Starr, 1991: An observational and theoretical study of highly supercooled altocumulus. *J. Atmos. Sci.,* **48,** 923–945.

Hobbs, P. V., and D. G. Atkinson, 1976: The concentrations of ice particles in orographic clouds and cyclonic storms over the Cascade Mountains. *J. Atmos. Sci.,* **33,** 1362–1374.

——, and A. L. Rangno, 1985: Ice particle concentrations in clouds. *J. Atmos. Sci.,* **42,** 2523–2549.

——, and ——, 1990: Rapid development of high ice particle concentrations in small Polar maritime cumuliform clouds. *J. Atmos. Sci.,* **47,** 2710–2722.

——, and ——, 1998: Microstructures of low and middle-level clouds over the Beaufort Sea. *Quart. J. Roy. Meteor. Soc.,* **124,** 2035–2071.

——, ——, M. D. Shupe, and T. Uttal, 2001: Airborne studies of cloud structures over the Arctic Ocean and comparisons with retrievals from ship-based remote sensing measurements. *J. Geophys. Res.,* **106,** 15 029–15 044.

Hogan, R. J., P. N. Francis, H. Flentje, A. J. Illingworth, M. Quante, and J. Pelon, 2003a: Characteristics of mixed-phase clouds. Part I: Lidar, radar and aircraft observations from CLARE '98. *Quart. J. Roy. Meteor. Soc.,* **129,** 2089–2116.

——, A. J. Illingworth, E. J. O'Connor, and J. P. V. Poiares Baptista, 2003b: Characteristics of mixed-phase clouds. Part II: A climatology from ground-based lidar. *Quart. J. Roy. Meteor. Soc.,* **129,** 2117–2134.

Intrieri, J. M., M. D. Shupe, T. Uttal, and B. J. McCarty, 2002: An annual cycle of Arctic cloud characteristics observed by radar and lidar at SHEBA. *J. Geophys. Res.,* **107,** 8030, doi:10.1029/2000JC000423.

Jiang, H., W. R. Cotton, J. O. Pinto, J. A. Curry, and M. J. Weiss-

bluth, 2000: Cloud resolving simulations of mixed-phase Arctic stratus observed during BASE: Sensitivity to concentration of ice crystals and large-scale heat and moisture advection. *J. Atmos. Sci.,* **57,** 2105–2117.

Khvorostyanov, V. I., J. A. Curry, I. Gultepe, and K. Strawbridge, 2003: A springtime cloud over the Beaufort Sea polynya: Three-dimensional simulation with explicit spectral microphysics and comparison with observations. *J. Geophys. Res.,* **108,** 4296, doi:10.1029/2001JD001489.

Korolev, A., and G. Isaac, 2003: Phase transformation of mixed-phase clouds. *Quart. J. Roy. Meteor. Soc.,* **129,** 19–38.

——, ——, S. G. Cober, J. W. Strapp, and J. Hallett, 2003: Microphysical characterization of mixed-phase clouds. *Quart. J. Roy. Meteor. Soc.,* **129,** 39–65.

Lawson, R. P., B. A. Baker, C. G. Schmitt, and T. L. Jensen, 2001: An overview of microphysical properties of Arctic clouds observed in May and July 1998 during FIRE ACE. *J. Geophys. Res.,* **106,** 14 989–15 014.

Liao, L., and K. Sassen, 1994: Investigation of relationships between Ka-band radar reflectivity and ice and liquid water content. *Atmos. Res.,* **34,** 231–248.

Lin, B., P. Minnis, and A. Fan, 2003: Cloud liquid water path variations with temperature observed during the Surface Heat Budget of the Arctic Ocean (SHEBA) experiment. *J. Geophys. Res.,* **108,** 4427, doi:10.1029/2002JD002851.

Mace, G. G., T. P. Ackerman, P. Minnis, and D. F. Young, 1998: Cirrus layer microphysical properties derived from surface-based millimeter radar and infrared interferometer data. *J. Geophys. Res.,* **103,** 23 207–23 216.

——, A. J. Heymsfield, and M. R. Poellot, 2002: On retrieving the microphysical properties of cirrus clouds using the moments of the millimeter-wavelength Doppler spectrum. *J. Geophys. Res.,* **107,** 4815, doi:10.1029/2001JD001308.

Matrosov, S. Y., 1997: Variability of microphysical parameters in high-altitude ice clouds: Result of the remote sensing method. *J. Appl. Meteor.,* **36,** 633–648.

——, 1999: Retrievals of vertical profiles of ice cloud microphysics from radar and IR measurements using tuned regressions between reflectivity and cloud parameters. *J. Geophys. Res.,* **104,** 16 741–16 753.

——, T. Uttal, J. B. Snider, and R. A. Kropfli, 1992: Estimation of ice cloud parameters from ground-based infrared radiometer and radar measurements. *J. Geophys. Res.,* **97,** 11 567–11 574.

——, A. V. Korolev, and A. J. Heymsfield, 2002: Profiling cloud ice mass and particle characteristic size from Doppler radar measurements. *J. Atmos. Oceanic Technol.,* **19,** 1003–1018.

Moran, K. P., B. E. Martner, M. J. Post, R. A. Kropfli, D. C. Welsh, and K. B. Widener, 1998: An unattended cloud-profiling radar for use in climate research. *Bull. Amer. Meteor. Soc.,* **79,** 443–455.

Morrison, H., M. D. Shupe, and J. A. Curry, 2003: Modeling clouds observed at SHEBA using a bulk microphysics parameterization implemented into a single-column model. *J. Geophys. Res.,* **108,** 4255, doi:10.1029/2002JD002229.

Moss, S. J., and D. W. Johnson, 1994: Aircraft measurements to validate and improve numerical model parameterizations of ice to water ratios in clouds. *Atmos. Res.,* **34,** 1–25.

Mossop, S. C., 1985: The origin and concentration of ice crystals in clouds. *Bull. Amer. Meteor. Soc.,* **66,** 264–273.

Olsson, P. Q., and J. Y. Harrington, 2000: Dynamics and energetics of the cloudy boundary layer in simulations of off-ice flow in the marginal ice zone. *J. Geophys. Res.,* **105,** 11 889–11 899.

Ose, T., 1993: An examination of the effects of explicit cloud water in the UCLA GCM. *J. Meteor. Soc. Japan,* **71,** 93–109.

Pinto, J. O., 1998: Autumnal mixed-phase cloudy boundary layers in the Arctic. *J. Atmos. Sci.,* **55,** 2016–2038.

——, J. A. Curry, and J. M. Intrieri, 2001: Cloud–aerosol interactions during autumn over Beaufort Sea. *J. Geophys. Res.,* **106** (D14), 15 077–15 097.

Pruppacher, H. R., and J. D. Klett, 1980: *Microphysics of Clouds and Precipitation.* D. Reidel, 454 pp.

Rauber, R. M., 1987: Characteristics of cloud ice and precipitation during wintertime storms over the mountains of northern Colorado. *J. Climate Appl. Meteor.,* **26,** 488–524.

——, and L. O. Grant, 1986: The characteristics and distribution of cloud water over the mountains of northern Colorado during winter storms. Part II: Spatial distribution and microphysical characteristics. *J. Climate Appl. Meteor.,* **25,** 489–504.

——, and A. Tokay, 1991: An explanation for the existence of supercooled water at the top of cold clouds. *J. Atmos. Sci.,* **48,** 1005–1023.

Sassen, K., 1984: Deep orographic cloud structure and composition derived from comprehensive remote sensing measurements. *J. Climate Appl. Meteor.,* **23,** 568–583.

——, 1987: Ice cloud content from radar reflectivity. *J. Climate Appl. Meteor.,* **26,** 1050–1053.

Shupe, M. D., and J. M. Intrieri, 2004: Cloud radiative forcing of the Arctic surface: The influence of cloud properties, surface albedo, and solar zenith angle. *J. Climate,* **17,** 616–628.

——, P. Kollias, S. Y. Matrosov, and T. L. Schneider, 2004: Deriving mixed-phase cloud properties from Doppler radar spectra. *J. Atmos. Oceanic Technol.,* **21,** 660–670.

——, T. Uttal, and S. Y. Matrosov, 2005: Arctic cloud microphysics retrievals from surface-based remote sensors at SHEBA. *J. Appl. Meteor.,* **44,** 1544–1562.

Smith, R. N. B., 1990: A scheme for predicting layer clouds and their water content in a general circulation model. *Quart. J. Roy. Meteor. Soc.,* **116,** 435–460.

Sun, Z., and K. P. Shine, 1994: Studies of the radiative properties of ice and mixed-phase clouds. *Quart. J. Roy. Meteor. Soc.,* **120,** 111–137.

——, and ——, 1995: Parameterization of ice cloud radiative properties and its application to the potential climatic importance of mixed-phase clouds. *J. Climate,* **8,** 1874–1888.

Tiedtke, M., 1993: Representation of clouds in large-scale models. *Mon. Wea. Rev.,* **121,** 3040–3061.

Tremblay, A., A. Glazer, W. Yu, and R. Benoit, 1996: A mixed-phase cloud scheme based on a single prognostic equation. *Tellus,* **48A,** 483–500.

Turner, D. D., 2005: Arctic mixed-phase cloud properties from AERI-lidar observations: Algorithm and results from SHEBA. *J. Appl. Meteor.,* **44,** 427–444.

Uttal, T., and Coauthors, 2002: Surface heat budget of the Arctic Ocean. *Bull. Amer. Meteor. Soc.,* **83,** 255–275.

Wang, Z., K. Sassen, D. N. Whiteman, and B. B. Demoz, 2004: Studying altocumulus with ice virga using ground-based active and passive remote sensors. *J. Appl. Meteor.,* **43,** 449–460.

Westwater, E. R., Y. Han, M. D. Shupe, and S. Y. Matrosov, 2001: Analysis of integrated cloud liquid and precipitable water vapor retrievals from microwave radiometers during SHEBA. *J. Geophys. Res.,* **106,** 32 019–32 030.

Zuidema, P., and Coauthors, 2005: An Arctic springtime mixed-phase cloudy boundary layer observed during SHEBA. *J. Atmos. Sci.,* **62,** 160–176.